

Hsa_circ_0074491 regulates the malignance of cholesteatoma keratinocytes by modulating the PI3K/Akt pathway by binding to miR-22-3p and miR-125a-5p

An observational study

Yunlong Hu, MM*^{id}, Xudong Qian, MM

Abstract

Cholesteatoma is a benign cystic lesion that can continue to grow like a tumor. Circular ribonucleic acid (RNA) hsa_circ_0074491 (circ_0074491) has been reported to be down-regulated in cholesteatoma tissues. However, the role and regulatory mechanism of circ_0074491 in the growth of cholesteatoma are unclear.

The expression of circ_0074491, microRNA (miR)-22-3p, and miR-125a-5p in cholesteatoma tissues was detected by quantitative real-time polymerase chain reaction. The proliferation, cell cycle, apoptosis, migration, and invasion of cholesteatoma keratinocytes were evaluated by 3-(4,5-dimethylthiazol-2-yl)-2,5-diphenyltetrazolium bromide, plate clone, flow cytometry, or transwell assays. Several protein levels were examined by western blotting. The targeting relationship between miR-22-3p or miR-125a-5p and circ_0074491 was verified via dual-luciferase reporter and RNA pull-down assays.

We observed the downregulation of circ_0074491 in cholesteatoma tissues. Furthermore, circ_0074491 knockdown facilitated cell proliferation, migration, invasion, and repressed cell apoptosis in cholesteatoma keratinocytes. Circ_0074491 was verified as a decoy for miR-22-3p and miR-125a-5p in cholesteatoma keratinocytes. Both miR-22-3p and miR-125a-5p silencing reversed the impacts of circ_0074491 silencing on proliferation, apoptosis, migration, and invasion of cholesteatoma keratinocytes. Also, circ_0074491 knockdown activated the PI3K/Akt pathway in cholesteatoma keratinocytes via miR-22-3p and miR-125a-5p.

Circ_0074491 played a suppressive role in cholesteatoma through inactivating the PI3K/Akt pathway via binding to miR-22-3p and miR-125a-5p, which provided a novel evidence for the involvement of circRNA in the development of cholesteatoma.

Abbreviations: circ_0074491 = circular RNA hsa_circ_0074491, circRNAs = circular RNAs, miR = microRNA, PPARGC1B = peroxisome proliferator-activated receptor gamma co-activator 1 beta, qRT-PCR = quantitative real-time polymerase chain reaction.

Keywords: cholesteatoma, circ_0074491, keratinocytes, miR-125a-5p, miR-22-3p

Editor: Jie Li.

The authors have no funding and conflicts of interest to disclose.

The datasets generated during and/or analyzed during the current study are not publicly available, but are available from the corresponding author on reasonable request.

Department of Otolaryngology, Anhui No.2 Provincial People's Hospital, No.1868 Dangshan Road, Hefei, Anhui, China.

* Correspondence: Yunlong Hu, Department of Otolaryngology, Anhui No.2 Provincial People's Hospital, No.1868 Dangshan Road, Hefei 230041, Anhui, China (e-mail: enthy88@163.com).

Copyright © 2021 the Author(s). Published by Wolters Kluwer Health, Inc. This is an open access article distributed under the terms of the Creative Commons Attribution-Non Commercial License 4.0 (CCBY-NC), where it is permissible to download, share, remix, transform, and buildup the work provided it is properly cited. The work cannot be used commercially without permission from the journal.

How to cite this article: Hu Y, Qian X. Hsa_circ_0074491 regulates the malignance of cholesteatoma keratinocytes by modulating the PI3K/Akt pathway by binding to miR-22-3p and miR-125a-5p: an observational study. *Medicine* 2021;100:37(e27122).

Received: 5 March 2021 / Received in final form: 12 August 2021 / Accepted: 16 August 2021

<http://dx.doi.org/10.1097/MD.00000000000027122>

Key points

1. Circ_0074491 was down-regulated in cholesteatoma tissues.
2. Silencing of circ_0074491 repressed apoptosis and accelerated proliferation, migration, and invasion of cholesteatoma keratinocytes.
3. Circ_0074491 was identified as a decoy for miR-22-3p and miR-125a-5p in cholesteatoma keratinocytes.
4. Circ_0074491 regulated the PI3K/Akt pathway in cholesteatoma keratinocytes.

1. Introduction

Cholesteatoma is a chronic middle ear disease, which is a benign cystic lesion in pathology.^[1] It can cause dizziness, tinnitus, hearing loss, facial paralysis, and brain abscesses by continuing to grow and destroy adjacent bone structures.^[2] Currently, surgery is the only way to treat cholesteatoma, but it usually recurs.^[3,4]

Therefore, there is a need to develop non-surgical treatment alternatives for cholesteatoma based on molecular mechanisms.^[5]

Circular RNAs (circRNAs) are characterized by a covalently closed continuous loop without a 5' or 3' polarities structure.^[6] They are resistant to RNase R and exhibit tissue-specific or cell-type-specific patterns.^[7] The molecular functions of circRNAs can be used as microRNA (miR) decoys, transcription regulators, and protein-like regulators.^[8] Mounting studies have demonstrated that circRNAs were connected with a series of diseases, such as cardiovascular diseases,^[9] neurodegenerative disorders,^[10] and cancers.^[11] Microarray analysis revealed that circRNAs had significant differential expression in cholesteatoma tissues relative to normal skin tissues, manifesting that circRNAs might exert a key role in cholesteatoma.^[12] Circular ribonucleic acid (RNA) hsa_circ_0074491 (circ_0074491) located at chr5:149215825-149221940, is derived from the peroxisome proliferator-activated receptor gamma co-activator 1 beta (PPARGC1B) gene (exon 8, 9, 10) and its splicing length is 1009 bp. It was reported that circ_0074491 expression was down-regulated in cholesteatoma^[12] and systemic lupus erythematosus.^[13] However, the role and regulatory mechanism of circ_0074491 in cholesteatoma are indistinct.

MiRs, another type of non-coding RNAs, are involved in the regulation of a range of cellular biological processes.^[14] It has reported that endogenous circRNAs could work as miR decoys.^[15] For example, circRNA DMNT3B downregulation facilitates vascular dysfunction via functioning as a miR-20b-5p decoy in diabetic retinal.^[16] Through starbase and circbank database predictions and preliminary experiments, we found that circ_0074491 may be the bait for miR-22-3p and miR-125a-5p. Many researches have reported that miR-22-3p^[17-19] and miR-125a-5p^[20-22] exert anti-tumor activity in a range of cancers. Nevertheless, whether circ_0074491 regulates cholesteatoma progression via miR-22-3p and miR-125a-5p is indistinct.

In the present study, we proved that circ_0074491 exerted a suppressive role in cholesteatoma. Moreover, circ_0074491 regulated cholesteatoma progression via the PI3K/Akt pathway via binding to miR-22-3p and miR-125a-5p.

2. Materials and methods

2.1. Patient tissue specimens

The study was approved by the Ethics Committee of Anhui No.2 Provincial People's Hospital. Twenty-eight paired cholesteatoma tissues and normal retroauricular kin tissues were obtained from cholesteatoma patients who had undergone surgery at Anhui No.2 Provincial People's Hospital. All patients had signed written informed consents prior to surgery.

2.2. Cell culture and transfection

To obtain cholesteatoma keratinocytes, we first put the cholesteatoma tissues in Keratinocyte-Serum Free Medium (5 mL) (AMS Biotechnology, Abingdon, Oxfordshire, UK). Next, the cholesteatoma tissues were treated with 20 mg/mL collagenase (0.5 mL, Sigma, St Louis, MO) to obtain single cells. After centrifugation (287 × g, 5 minutes), the pellets were re-suspended in Keratinocyte-Serum Free Medium (10 mL) supplemented with streptomycin/penicillin (Solarbio, Beijing, China) and grown at 37°C in a moist atmosphere with 5% CO₂.

Cholesteatoma keratinocytes were transfected with oligonucleotides or vectors using Lipofectamine 3000 reagent (Thermo Fisher Scientific, Waltham, MA). Small interfering RNA (si) targeting circ_0074491 and its negative control (si-NC) were synthesized by Geneseeed (Guangzhou, China). The sequence of circ_0074491 was cloned into the pCD5-ciR vectors (Geneseeed) to obtain the pCD5-ciR-circ_0074491 vectors (circ_0074491). MiR-22-3p mimic (miR-22-3p), miR-125a-5p mimic (miR-125a-5p), miR-22-3p inhibitor (anti-miR-22-3p), miR-125a-5p inhibitor (anti-miR-125a-5p), and their negative controls (miR-NC and anti-miR-NC) were purchased from GenePharma (Shanghai, China).

2.3. Quantitative real-time polymerase chain reaction

For total RNA (tissue specimens and cholesteatoma keratinocytes) isolation, we used Trizol reagent (Sigma) according to the manufacturer's instructions. After treatment with DNase I (Sigma), the isolated total RNA was quantified at the ratio of A260/A280. Total RNA was reversely transcribed with the M-MLV Reverse Transcriptase (Promega, Madison, WI) or miScriptIIRT kit (Qiagen, San Diego, CA). Quantitative real-time polymerase chain reaction (qRT-PCR) was executed with the SYBR Green PCR Master Mix (Thermo Fisher Scientific). The data were analyzed by the 2^{-ΔΔCt} method. The primers utilized in the study were listed in Table 1. Glyceraldehyde-3-phosphate

Table 1

Primer sequences for qRT-PCR.

| Genes | Primer sequences (5'-3') |
|------------------|--|
| circ_0074491 | Forward (F): 5'-GGGAAAAGGCCATTGGGGAA-3' Reverse (R): 5'-GGTGGGGTGGAGTCCCTCTATT-3' |
| miR-22-3p | F: 5'-GCGAAGCTGCCAGTTGAAG-3' R: 5'-AGTGCAGGGTCCGAGGTATT-3' |
| miR-125a-5p | F: 5'-GCGTCCCTGAGACCCCTTAAC-3' R: 5'-AGTGCAGGGTCCGAGGTATT-3' |
| miR-485-5p | F: 5'-CGAGAGGCTGGCCGTGAT-3' R: 5'-AGTGCAGGGTCCGAGGTATT-3' |
| miR-125b-5p | F: 5'-GCGTCCCTGAGACCCCTAAC-3' R: 5'-AGTGCAGGGTCCGAGGTATT-3' |
| miR-34a-5p | F: 5'-GCGGTGGCAGTGTCTTAGCT-3' R: 5'-AGTGCAGGGTCCGAGGTATT-3' |
| miR-6852-3p | F: 5'-GCGCGTGTCTCTGT-3' R: 5'-AGTGCAGGGTCCGAGGTATT-3' |
| miR-6884-5p | F: 5'-GCGGAGAGGCTGAGAAGGTG-3' R: 5'-AGTGCAGGGTCCGAGGTATT-3' |
| GAPDH | F: 5'-GATTCCACCATGGCAAATTC-3' R: 5'-TCGCTCCTGGAAAGTGGTAT-3' |
| U6 | F: 5'-CTCGCTTCGGCAGCACA-3' R: 5'-AACGCTTCACGAATTTGCGT-3' |
| hsa_circ_0011385 | Forward (F): 5'-TGACAACAATGAGCCCTACA-3' Reverse (R): 5'-TTTCTTGGCACTATACTGG-3' |
| EIF3I | F: 5'-GGCCATGAGCGGTCCATTAC-3' R: 5'-ACATTGACGATAGGGTCCCTTGG-3' |
| PRDX6 | F: 5'-GACTCATGGGGCATTCTCTC-3' R: 5'-CAAGCTCCCGATTCTATATC-3' |
| β-Actin | F: 5'-GCACCACACCTTCTACAATG-3' R: 5'-TGCTTGTCTGATCCACATCTG-3' |
| miR149-5p | F: 5'-TCTGGCTCCGTGTCTTCACTCCC-3' R: 5'-TATGGTTGTTCTGCTCTCTGTGTG-3' |
| 18 SrRNA | F: 5'-GGAGTATGTTGCAAAGCTGA-3' R: 5'-ATCTGTCAATCCTGTCCGTGT-3' |
| U6 | F: 5'-GCATGACGTCTGCTTTGGA-3' R: 5'-CCACAATCATTCTGCCATCA-3' |

circ_0074491 = circular RNA hsa_circ_0074491, miR = microRNA, qRT-PCR = quantitative real-time polymerase chain reaction.

dehydrogenase (GAPDH) or U6 small nuclear RNA (U6) was used as an internal.

2.4. Cell proliferation assay

The transfected cholesteatoma keratinocytes were seeded into 96-well plates and maintained for 24 hours, 48 hours, or 72 hours. Then, the 3-(4, 5-dimethylthiazol-2-yl)-2, 5-diphenyltetrazolium bromide (MTT) solution (20 μ L, Sigma) was added into each well. After incubation for 4 hours, dimethyl sulfoxide (150 μ L, Sigma) was employed to dissolve the precipitated crystals. Subsequently, the absorbance at 570 nm was analyzed using a microplate reader (BMG LABTECH, Offenburg, Germany).

2.5. Plate clone assay

The transfected cholesteatoma keratinocytes were seeded into 6-well plates and grown for 2 weeks. Then, the cells were fixed by paraformaldehyde (4%, Sigma) and stained with crystal violet (0.5%, Solarbio). The number of colonies (containing more than 50 cells) was figured and photographed with an inverted microscope (MTX Lab Systems, Bradenton, FL).

2.6. Cell cycle analysis

The transfected cholesteatoma keratinocytes (1×10^6) were harvested and treated with trypsin to obtain single cells. Afterwards, the cells were fixed by ethanol (75%) at 4°C for 4 hours. Then, the cells were incubated with propidium iodide (PI) (50 μ g/mL, Solarbio) and RNase A (100 μ g/mL, Solarbio). The fluorescence-activated cell sorting (FACS) Calibur (BD Biosciences, San Jose, CA) was utilized for the detection of the cell distribution. Experimental data were analyzed with the FACS Diva (BD Biosciences).

2.7. Cell apoptosis analysis

The apoptotic rate of the transfected cholesteatoma keratinocytes was determined using the FACS Calibur (BD Biosciences) with the Annexin V-Fluorescein Isothiocyanate (AV-FITC)/PI Apoptosis Detection kit (Solarbio). In short, the cells were collected and re-suspended in binding buffer. The cells were then stained with AV-FITC and PI. After detection with the FACS Calibur (BD Biosciences), the data were evaluated using the FACS Diva (BD Biosciences).

2.8. Western blotting

Antibodies related to PI3K/Akt pathway were purchased from Cell Signaling Technology (Santa Cruz, California), and the remaining antibodies were bought from Abcam, Cambridge, MA. GAPDH was used as a loading control. In brief, total protein was extracted from the transfected cholesteatoma keratinocytes using the RIPA buffer containing a protease inhibitor cocktail (MedChem Express, Shanghai, China). Total protein was then isolated using sodium dodecyl sulfate-polyacrylamide gel electrophoresis (10%, SDS-PAGE, Sangon Biotech, Shanghai, China) and transferred onto polyvinylidene difluoride (PVDF) membranes (Sigma). Afterwards, the membranes were blocked in tris buffered saline tween (TBST) buffer containing 5% skim milk. Thereafter, the membranes were incubated with primary antibodies against GAPDH (ab181602, 1:10,000), B-cell lym-

phoma/leukaemia-2 (Bcl-2) (ab32124, 1:1000), Bcl-2-associated x (Bax) (ab182733, 1:2000), matrix metalloproteinase 2 (MMP2) (ab181286, 1:1000), matrix metalloproteinase 9 (MMP9) (ab38898, 1:1000), phosphatidylinositol 3-kinase (PI3K) (#4257, 1:1000), phosphorylated (p)-PI3K (#17366, 1:1000), serine/threonine kinase 1 (Akt) (#9272, 1:1000), and p-Akt (#9611, 1:1000). Afterwards, the membranes were incubated with goat anti-rabbit IgG (ab6721, 1:10,000). The immunoblots were visualized with the enhanced chemiluminescence solution (Beyotime, Shanghai, China).

2.9. Cell migration and invasion analysis

In brief, 200 μ L Keratinocyte-Serum Free Medium containing the transfected cholesteatoma keratinocytes (1×10^5 cells) was added to the upper chamber of the transwell (Costar, Cambridge, MA). The bottom of the transwell chamber was supplemented with 600 μ L Keratinocyte-Serum Free Medium containing FBS (10%, Sigma). The migrated and invaded cells were fixed with paraformaldehyde (4%, Sigma) and stained with crystal violet (0.25%, Solarbio). The upper chamber of the transwell used in the invasion assay was pre-coated with matrigel (Sigma), but the migration assay did not. An inverted microscope (MTX Lab Systems) at 100 \times magnification was applied to calculate and photograph the migrated and invaded cells.

2.10. Bioinformatics analysis

The binding sites between circ_0074491 and miRs were predicted with the circBank (<http://www.circbank.cn/>) database and starbase (<http://starbase.sysu.edu.cn/>).

2.11. RNA pull-down assay

The biotinylated-circ_0074491 probe (circ_0074491 probe) and its negative control NC probe were obtained from (Genesee). In short, the circ_0074491 probe was incubated with streptavidin C-1 magnetic beads (Thermo Fisher Scientific) to construct the probe-coated beads. The lysate of cholesteatoma keratinocytes and probe-coated beads were co-incubated at 4°C for overnight. The enrichment of circ_0074491 and miRs (miR-485-5p, miR-125b-5p, miR-22-3p, miR-34a-5p, miR-125a-5p, miR-6852-3p, and miR-6884-5p) was evaluated with qRT-PCR.

2.12. Dual-luciferase reporter assay

The cholesteatoma keratinocytes were cotransfected with miR-22-3p, miR-125a-5p, or miR-NC and luciferase vectors carrying circ_0074491 WT or circ_0074491 MUT. Subsequently, the relative luciferase intensity (the ratio of Firefly luciferase activity to Renilla luciferase activity) was analyzed by luciferase reporter assay kit (Promega). The luciferase reporter vectors containing circ_0074491 wild type (WT) or circ_0074491 mutant (MUT) was established by Genechem (Shanghai, China).

2.13. Statistical analysis

The Statistical Package for the Social Sciences version 20.0 software (SPSS, Inc., Chicago, IL) was utilized for statistical analysis. The above experiments were carried out at least 3 times. Data were expressed as mean \pm standard deviation. Independent or paired Student *t* test was employed to analyze the difference

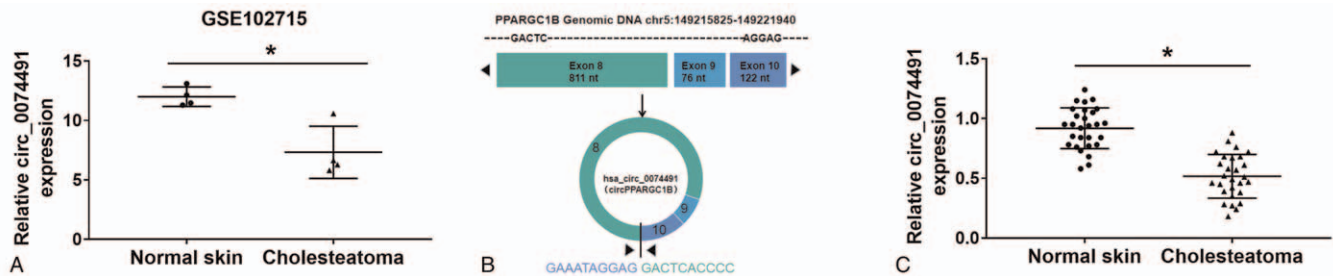


Figure 1. Expression pattern of circ_0074491 in cholesteatoma. (A) Microarray data (GEO accession: GSE102715) analysis of the differential expression level of circ_0074491 in cholesteatoma tissues and normal retroauricular skin tissues. (B) Schematic diagram illustrated the formation of circ_0074491 originated from the PPARGC1B gene (exon 8, 9, 10). (C) QRT-PCR exhibited the expression of in 28 paired cholesteatoma tissues and normal retroauricular skin tissues. * $P < .05$. Circ_0074491 = circular RNA hsa_circ_0074491, PPARGC1B = peroxisome proliferator-activated receptor gamma co-activator 1 beta, qRT-PCR = quantitative real-time polymerase chain reaction

between 2 groups. Differences were considered statistically significant for $P < .05$. One-way variance analysis (ANOVA) with Turkey post hoc test was applied to determine the differences among 3 or more groups.

3. Results

3.1. Circ_0074491 had lower expression in cholesteatoma

To screen for differentially expressed circRNAs in cholesteatoma, we analyzed the microarray data (GEO accession: GSE102715) and discovered that circ_0074491 expression was reduced in cholesteatoma tissues in comparison to normal retroauricular skin tissues (Fig. 1A). Circ_0074491 arises from the PPARGC1B gene (exon 8, 9, 10), which is located at chr5:149215825-149221940 (Fig. 1B). To verify the expression pattern of circ_0074491 in cholesteatoma, we detected the level of circ_0074491 in 28 paired cholesteatoma tissues and normal retroauricular skin tissues. QRT-PCR exhibited that circ_0074491 expression was apparently decreased in cholesteatoma tissues than that in normal retroauricular skin tissues (Fig. 1C). These data indicated that low circ_0074491 expression might be involved in the growth of cholesteatoma.

3.2. Silencing of circ_0074491 reduced cell cycle arrest, apoptosis, accelerated proliferation, colony formation, migration, and invasion of cholesteatoma keratinocytes

To analyze the biological role of circ_0074491 in cholesteatoma in vitro, we successfully isolated cholesteatoma keratinocytes from cholesteatoma tissues. Then, we explored the role of circ_0074491 in cholesteatoma keratinocytes through loss-of-function experiments. As exhibited in Figure 2A, circ_0074491 expression was overtly reduced in cholesteatoma keratinocytes after si-circ_0074491 transfection compared to the control si-NC. MTT assay exhibited that circ_0074491 silencing accelerated cell proliferation in cholesteatoma keratinocytes (Fig. 2B). Plate clone assay exhibited that the number of colony formation of circ_0074491-inhibited cholesteatoma keratinocytes was apparently elevated compared to the control group (Fig. 2C). Cell cycle analysis presented that silenced circ_0074491 expression reduced the number of cholesteatoma keratinocytes in G0/G1 stage and increased the number of cholesteatoma keratinocytes in S stage, implying that circ_0074491 downregulation accelerated cell cycle progression in cholesteatoma keratinocytes

(Fig. 2D). Cell apoptosis analysis exhibited that the apoptotic rate of cholesteatoma keratinocytes was reduced after si-circ_0074491 transfection (Fig. 2E). Moreover, circ_0074491 knockdown reduced the level of Bax and elevated the level of Bcl-2 in cholesteatoma keratinocytes (Fig. 2F). Transwell assay manifested that circ_0074491 silencing could facilitate the migration and invasion of cholesteatoma keratinocytes (Fig. 2G and H). Also, the levels of MMP2 and MMP9 were up-regulated in circ_0074491-silenced cholesteatoma keratinocytes (Fig. 2I). Together, these results manifested that circ_0074491 silencing accelerated the malignancy of cholesteatoma keratinocytes.

3.3. Circ_0074491 acted as a decoy for miR-22-3p and miR-125a-5p in cholesteatoma keratinocytes

To survey the regulatory mechanism of circ_0074491 in cholesteatoma, we predicted possible miRs with complementary sites to circ_0074491 using starbase and circbank databases. As shown in Figure 3A, 7 miRs (miR-485-5p, miR-125b-5p, miR-22-3p, miR-34a-5p, miR-125a-5p, miR-6852-3p, and miR-6884-5p) with complementary sites to circ_0074491 were simultaneously presented in the starbase and circbank databases. RNA pull-down assay exhibited that circ_0074491 could be pulled down by circ_0074491 probe when compared with the NC probe in cholesteatoma keratinocytes transfected with vector or circ_0074491 (Fig. 3B). Of these 7 miRs, only 2 miRs (miR-22-3p and miR-125a-5p) could be pulled down by circ_0074491 probe in cholesteatoma keratinocytes (Fig. 3C). The presumptive binding sites between circ_0074491 and miR-22-3p or miR-125a-5p were exhibited in Figure 3D. Dual-luciferase reporter assay manifested that both miR-22-3p and miR-125a-5p mimics could reduce the luciferase activity of the luciferase vectors carrying circ_0074491 WT compared to the control miR-NC in cholesteatoma keratinocytes, while there was no distinct change in the luciferase vectors carrying circ_0074491 MUT (Fig. 3E and F). We also observed that the levels of miR-22-3p and miR-125a-5p were distinctly up-regulated in cholesteatoma tissues than that in normal retroauricular skin tissues (Fig. 3G and H). Also, inhibited circ_0074491 expression could elevate the expression of miR-22-3p and miR-125a-5p in cholesteatoma keratinocytes (Fig. 3I). In sum, these data suggested that circ_0074491 served as a decoy for miR-22-3p and miR-125a-5p in cholesteatoma keratinocytes.

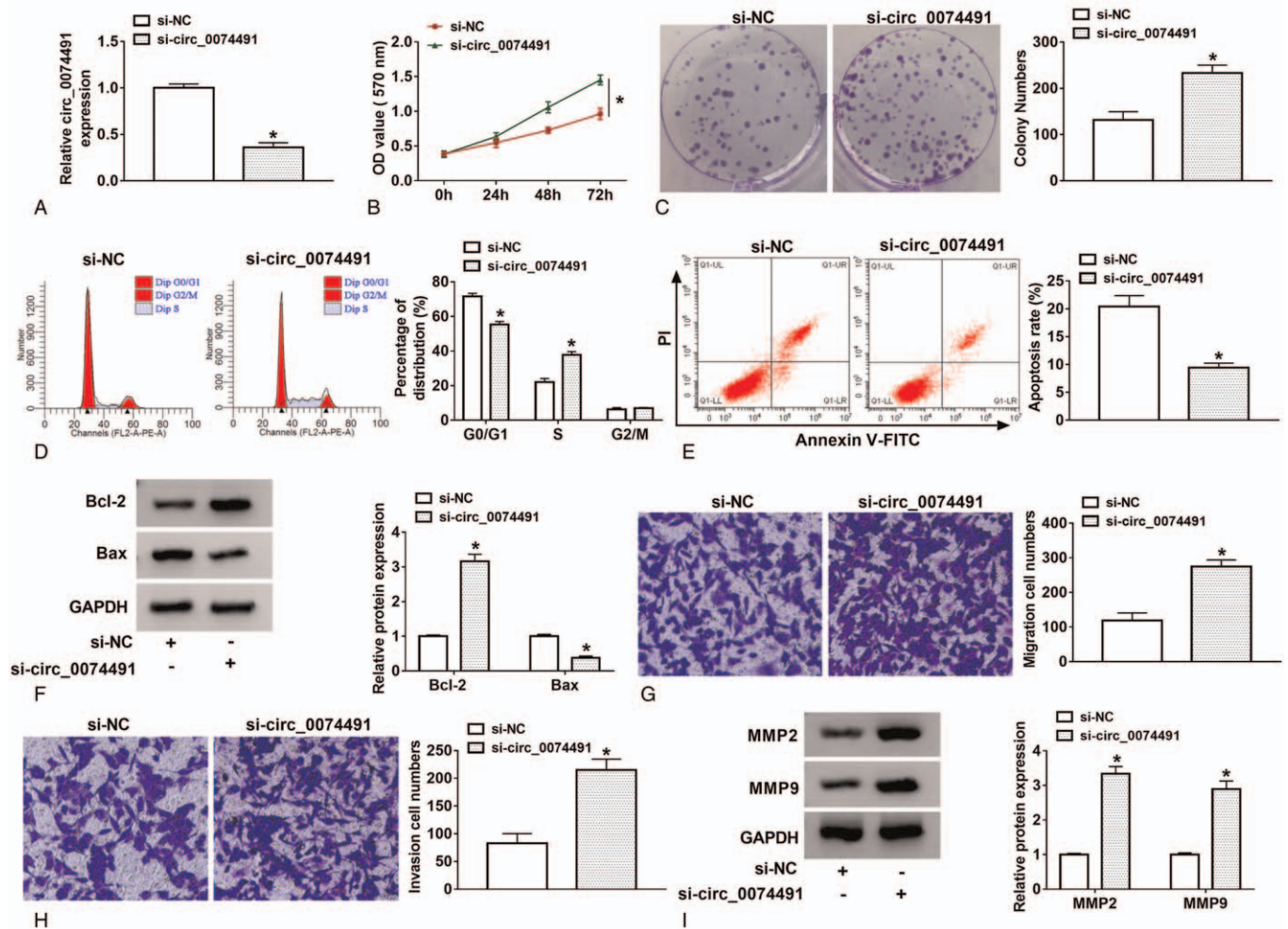


Figure 2. Circ_0074491 knockdown contributed to the malignancy of cholesteatoma keratinocytes. (A–I) Cholesteatoma keratinocytes were transfected with si-NC or si-circ_0074491. (A) The transfection efficiency of circ_0074491 silencing was analyzed by qRT-PCR. (B–E) The proliferation, colony formation, cell cycle progression, and apoptosis of cholesteatoma keratinocytes were determined by MTT, plate clone, or flow cytometry assays. (F) The levels of Bcl-2 and Bax in cholesteatoma keratinocytes were examined using western blotting. (G and H) The migration and invasion of cholesteatoma keratinocytes were evaluated using transwell assay. (I) The levels of MMP2 and MMP9 in cholesteatoma keratinocytes were detected by western blotting. * $P < .05$. Circ_0074491 = circular RNA hsa_circ_0074491, qRT-PCR = quantitative real-time polymerase chain reaction.

3.4. Both miR-22-3p and miR-125a-5p inhibitors reversed circ_0074491 knockdown-mediated influence on the malignant behaviors of cholesteatoma keratinocytes

Based on the above findings, we further surveyed whether circ_0074491 regulated the malignant behaviors of cholesteatoma keratinocytes through miR-22-3p and miR-125a-5p. QRT-PCR exhibited that circ_0074491 silencing could elevate the expression of miR-22-3p in cholesteatoma keratinocytes, but this increase was overturned after anti-miR-22-3p or anti-miR-22-3p/125a-5p transfection (Fig. 4A). Furthermore, knockdown of circ_0074491 increased miR-125a-5p expression in cholesteatoma keratinocytes, while this influence was overturned after transfection with anti-miR-125a-5p or anti-miR-22-3p/125a-5p (Fig. 4B). Also, the accelerative influence of circ_0074491 inhibition on proliferation, colony formation, and cell cycle progression of cholesteatoma keratinocytes was partly abolished by the silencing of miR-22-3p and/or miR-125a-5p (Fig. 4C–E). Moreover, the inhibitory role of circ_0074491 silencing on apoptosis of cholesteatoma keratinocytes was reversed by miR-22-3p and/or miR-125a-5p knockdown (Fig. 4F). Both the

upregulation of Bcl-2 and the downregulation of Bax in cholesteatoma keratinocytes caused by circ_0074491 knockdown were restored after miR-22-3p and/or miR-125a-5p knockdown (Fig. 4G). In addition, miR-22-3p or/and miR-125a-5p silencing could overturn the facilitation of migration and invasion of cholesteatoma keratinocytes mediated by circ_0074491 knockdown (Fig. 4H and I). We also observed that miR-22-3p and/or miR-125a-5p knockdown could partly reverse the upregulation of MMP2 and MMP9 in cholesteatoma keratinocytes induced by the repression of circ_0074491 (Fig. 4J). These findings suggested that circ_0074491 regulated the malignant behaviors of cholesteatoma keratinocytes via miR-22-3p and miR-125a-5p.

3.5. Circ_0074491 modulated the PI3K/Akt pathway via miR-22-3p and miR-125a-5p in cholesteatoma keratinocytes

Previous study revealed that the PI3K/Akt pathway was involved in cholesteatoma.^[23] Subsequently, we employed western

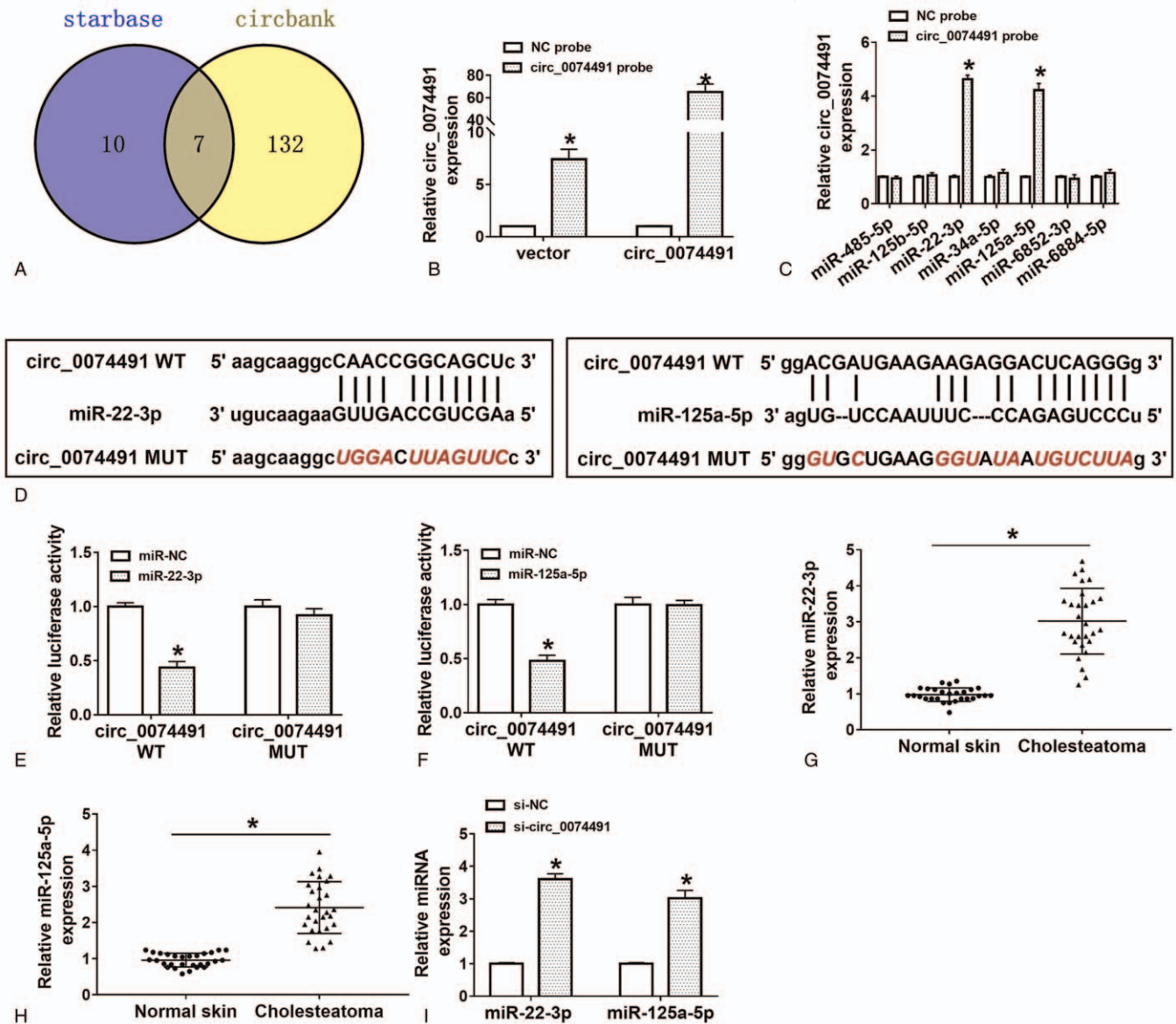


Figure 3. Circ_0074491 was verified as a decoy for miR-22-3p and miR-125a-5p in cholesteatoma keratinocytes. (A) The possible miRNAs (miR-485-5p, miR-125b-5p, miR-22-3p, miR-34a-5p, miR-125a-5p, miR-6852-3p, and miR-6884-5p) with complementary sites to circ_0074491 were predicted by starbase and circbank databases. (B) QRT-PCR revealed whether circ_0074491 could be pulled down by circ_0074491 probe or NC probe in cholesteatoma keratinocytes transfected with vector or circ_0074491. (C) QRT-PCR exhibited whether the predicted 7 miRNAs could be pulled down by circ_0074491 probe or NC probe in cholesteatoma keratinocytes. (D) Schematic diagram illustrated the presumptive binding sites between circ_0074491 and miR-22-3p or miR-125a-5p. (E and F) Dual-luciferase reporter assay was conducted to verify the relationship between circ_0074491 and miR-22-3p or miR-125a-5p in cholesteatoma keratinocytes. (G and H) Expression levels of miR-22-3p and miR-125a-5p in cholesteatoma tissues and normal retroauricular skin tissues were surveyed by qRT-PCR. (I) The expression of miR-22-3p and miR-125a-5p in cholesteatoma keratinocytes transfected with si-NC or si-circ_0074491 was measured by qRT-PCR. **P* < .05. Circ_0074491 = circular RNA hsa_circ_0074491, miR = microRNA, qRT-PCR = quantitative real-time polymerase chain reaction.

blotting to investigate whether circ_0074491 modulated the malignant behaviors of cholesteatoma keratinocytes via regulating the PI3K/Akt pathway via miR-22-3p and miR-125a-5p. The results exhibited that circ_0074491 knockdown could elevate the levels of p-PI3K and p-Akt in cholesteatoma keratinocytes, but this elevation was overturned after miR-22-3p and/or miR-125a-5p silencing (Fig. 5). These data indicated that circ_0074491 regulated the PI3K/Akt pathway through adsorbing miR-22-3p and miR-125a-5p in cholesteatoma keratinocytes.

4. Discussion

Recently, circRNAs were discovered to be abnormally expressed in human diseases.^[24] Increasing evidence proved that circRNAs might be diagnostic markers and therapeutic targets for some diseases.^[25,26] Gao et al^[12] revealed that there were 355 observably differentially expressed circRNAs in cholesteatoma, including circ_0074491. However, the regulatory mechanism by which circ_0074491 affects the advancement of cholesteatoma is unclear.

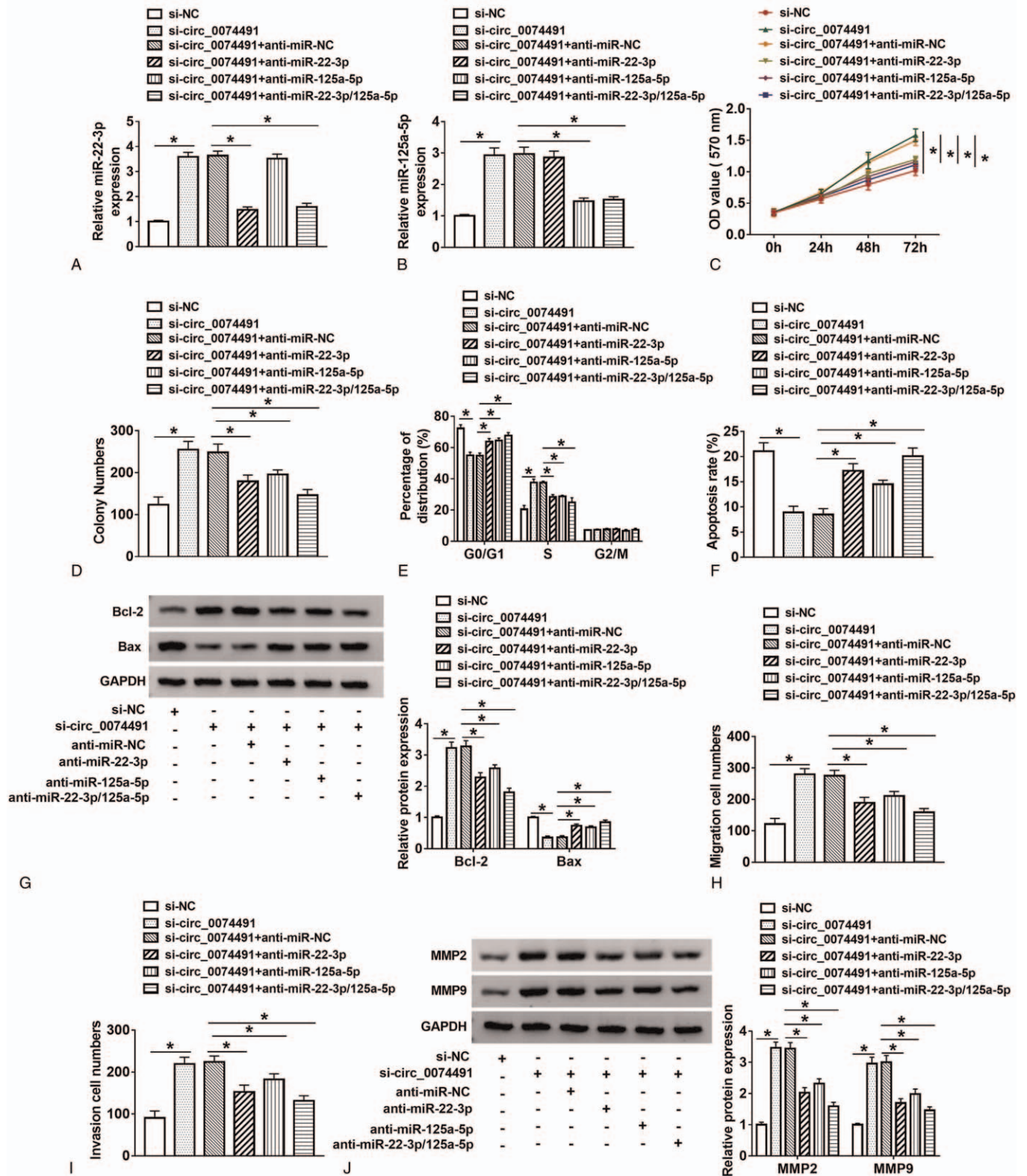


Figure 4. Circ_0074491 exerted a role in cholesteatoma keratinocytes via miR-22-3p and miR-125a-5p. (A–J) Cholesteatoma keratinocytes were transfected with si-NC, si-circ_0074491, si-circ_0074491+anti-miR-NC, si-circ_0074491+anti-miR-22-3p, si-circ_0074491+anti-miR-125a-5p, or si-circ_0074491+anti-miR-22-3p/125a-5p. (A and B) QRT-PCR was executed to assess the expression of miR-22-3p and miR-125a-5p in cholesteatoma keratinocytes. (C–F) MTT, plate clone, or flow cytometry assays was performed to determine the proliferation, colony formation, cell cycle progression, and apoptosis of cholesteatoma keratinocytes. (G) Western blotting was employed to survey the levels of Bcl-2 and Bax in cholesteatoma keratinocytes. (H and I) Transwell assay was conducted to analyze the migration and invasion of cholesteatoma keratinocytes. (J) Western blotting was performed for the detection of the levels of MMP2 and MMP9 in cholesteatoma keratinocytes. **P* < .05. Circ_0074491 = circular RNA hsa_circ_0074491, miR = microRNA, qRT-PCR = quantitative real-time polymerase chain reaction.

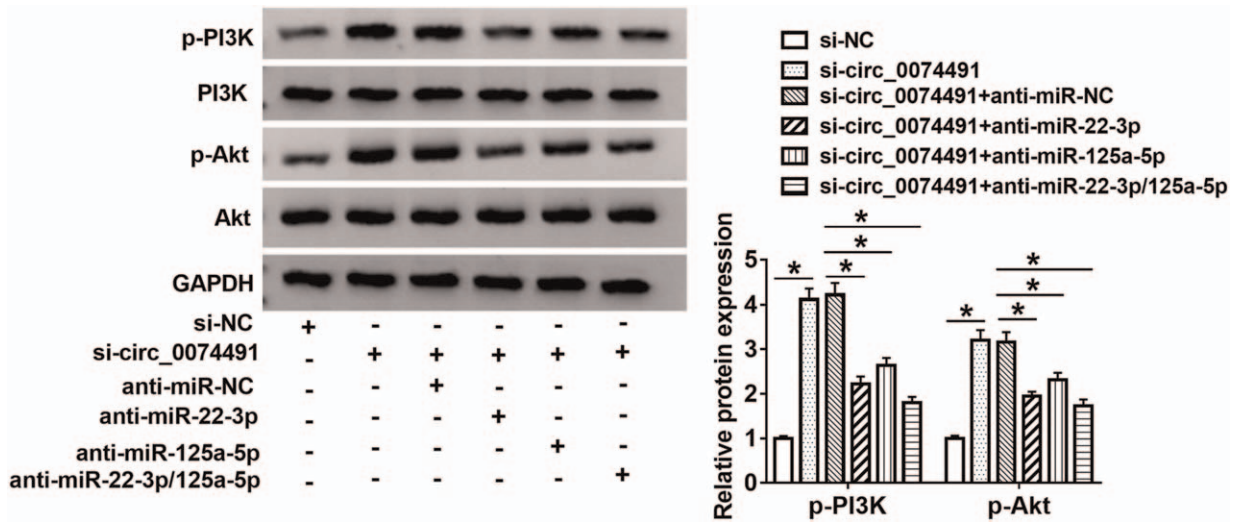


Figure 5. Circ_0074491 regulated the PI3K/Akt pathway by miR-22-3p and miR-125a-5p in cholesteatoma keratinocytes. The levels of p-PI3K, PI3K, p-Akt, or Akt in cholesteatoma keratinocytes transfected with si-NC, si-circ_0074491, si-circ_0074491+anti-miR-NC, si-circ_0074491+anti-miR-22-3p, si-circ_0074491+anti-miR-125a-5p, or si-circ_0074491+anti-miR-22-3p/125a-5p were measured by western blotting. * $P < .05$. Circ_0074491 = circular RNA hsa_circ_0074491, miR = microRNA.

The gene symbol of circ_0074491 is PPARGC1B. It was reported that PPARGC1B could facilitate the differentiation of anti-inflammatory macrophages and repress the expression of diverse cytokines.^[27] In non-small cell lung cancer, PPARGC1B was proved to play a tumor suppressive role.^[28] In our study, we verified that circ_0074491 was down-regulated in cholesteatoma tissues. Furthermore, silenced circ_0074491 expression contributed to colony formation, proliferation, invasion, migration, and curbed apoptosis, cell cycle arrest of cholesteatoma keratinocytes. Therefore, these findings indicated that circ_0074491 overexpression could reduce the growth of cholesteatoma.

In the study, we discovered that circ_0074491 was a decoy for miR-22-3p and miR-125a-5p in cholesteatoma keratinocytes through online bioinformatics, dual-luciferase reporter, and RNA-pull down assays. MiR-22-3p was identified as a biomarker for schizophrenia.^[29] Forced miR-22-3p expression could relieve AD symptoms.^[30] Previous studies unmasked that miR-22-3p exerted a tumor inhibitory role in hepatocellular carcinoma,^[31] lung adenocarcinoma,^[18] and retinoblastoma,^[32] but it exerted a carcinogenic role in papillary thyroid cancer.^[33] For miR-125a-5p, it could improve hepatic glycolipid metabolism disorder in type 2 diabetes^[34] and act as a tumor suppressor in bladder cancer^[35] and breast cancer.^[36] Also, miR-125a-5p could contribute to osteoclastogenesis.^[37] Herein, miR-22-3p and miR-125a-5p expression were elevated in cholesteatoma tissues. Both miR-22-3p and miR-125a-5p inhibitors could overturn the influence of circ_0074491 knockdown on the malignancy of cholesteatoma keratinocytes. These data indicated that circ_0074491 regulated the malignancy of cholesteatoma keratinocytes via miR-22-3p and miR-125a-5p.

The PI3K/Akt pathway is considered to be a key regulatory node for many physiological processes.^[38] The activated PI3K/Akt pathway was demonstrated to exert a cancerigenic role in a series of tumors.^[39] Liu et al^[23] reported that cholesteatoma epithelial hyper-proliferation was associated with the activation of the EGFR/PI3K/Akt/cyclinD1 pathway. Yune and Byun^[40] also indicated that the activation of Akt might be connected with

cellular hyperplasia in cholesteatoma. Herein, we discovered that silencing of circ_0074491 activated the PI3K/Akt pathway through miR-22-3p and miR-125a-5p. All findings indicated that circ_0074491 regulated the malignancy of cholesteatoma keratinocytes via modulating the PI3K/Akt pathway via miR-22-3p and miR-125a-5p.

In sum, our study revealed the role and regulatory mechanism of circ_0074491 in cholesteatoma growth. We proved that the circ_0074491 downregulation facilitated the malignant behaviors of cholesteatoma keratinocytes via modulating the PI3K/Akt pathway through adsorbing miR-22-3p and miR-125a-5p, thereby providing a new mechanism for the understanding the advancement of cholesteatoma.

Author contributions

Conceptualization: Yunlong Hu.

Data curation: Yunlong Hu, Xudong Qian.

Formal analysis: Yunlong Hu, Xudong Qian.

Methodology: Yunlong Hu, Xudong Qian.

Project administration: Yunlong Hu, Xudong Qian.

Visualization: Xudong Qian.

Writing – original draft: Yunlong Hu, Xudong Qian.

Writing – review & editing: Yunlong Hu, Xudong Qian.

References

- [1] Kuo C-L, Shiao A-S, Yung M, et al. Updates and knowledge gaps in cholesteatoma research. *Biomed Res Int* 2015;2015:854024.
- [2] Hamed MA, Nakata S, Sayed RH, et al. Pathogenesis and bone resorption in acquired cholesteatoma: current knowledge and future perspectives. *Clin Exp Otorhinolaryngol* 2016;9:298–308.
- [3] van der Toom HFE, van der Schroeff MP, Pauw RJ. Single-stage mastoid obliteration in cholesteatoma surgery and recurrent and residual disease rates: a systematic review. *JAMA Otolaryngol Head Neck Surg* 2018;144:440–6.
- [4] Crowson MG, Ramprasad VH, Chapurin N, Cunningham CD, Kaylie DM. Cost analysis and outcomes of a second-look tympanoplasty-mastoidectomy strategy for cholesteatoma. *Laryngoscope* 2016;126:2574–9.

- [5] Xie S, Liu X, Pan Z, et al. Microarray analysis of differentially-expressed microRNAs in acquired middle ear cholesteatoma. *Int J Med Sci* 2018;15:1547–54.
- [6] Salzman J. Circular RNA expression: its potential regulation and function. *Trends Genet* 2016;32:309–16.
- [7] Li X, Yang L, Chen L-L. The biogenesis, functions, and challenges of circular RNAs. *Mol Cell* 2018;71:428–42.
- [8] Hsiao K-Y, Sun HS, Tsai S-J. Circular RNA - new member of noncoding RNA with novel functions. *Exp Biol Med (Maywood)* 2017;242:1136–41.
- [9] Fan X, Weng X, Zhao Y, Chen W, Gan T, Xu D. Circular RNAs in cardiovascular disease: an overview. *Biomed Res Int* 2017;2017:5135781.
- [10] D'Ambra E, Caputo D, Morlando M. Exploring the regulatory role of circular RNAs in neurodegenerative disorders. *Int J Mol Sci* 2019;20:331–9.
- [11] Chan JJ, Tay Y. Noncoding RNA:RNA regulatory networks in cancer. *Int J Mol Sci* 2018;19:331–9.
- [12] Gao J, Tang Q, Xue R, et al. Comprehensive circular RNA expression profiling with associated ceRNA network reveals their therapeutic potential in cholesteatoma. *Oncol Rep* 2020;43:1234–44.
- [13] Zhang J, Liu Y, Shi G. The circRNA-miRNA-mRNA regulatory network in systemic lupus erythematosus. *Clin Rheumatol* 2021;40:331–9.
- [14] Creugny A, Fender A, Pfeffer S. Regulation of primary microRNA processing. *FEBS Lett* 2018;592:1980–96.
- [15] Kulcheski FR, Christoff AP, Margis R. Circular RNAs are miRNA sponges and can be used as a new class of biomarker. *J Biotechnol* 2016;238:42–51.
- [16] Zhu K, Hu X, Chen H, et al. Downregulation of circRNA DMNT3B contributes to diabetic retinal vascular dysfunction through targeting miR-20b-5p and BAMBI. *EBioMedicine* 2019;49:341–53.
- [17] Hussein NA, Kholy ZA, Anwar MM, Ahmad MA, Ahmad SM. Plasma miR-22-3p, miR-642b-3p and miR-885-5p as diagnostic biomarkers for pancreatic cancer. *J Cancer Res Clin Oncol* 2017;143:83–93.
- [18] Dong HX, Wang R, Jin XY, Zeng J, Pan J. LncRNA DGCR5 promotes lung adenocarcinoma (LUAD) progression via inhibiting hsa-mir-22-3p. *J Cell Physiol* 2018;233:4126–36.
- [19] Gan L, Lv L, Liao S. Long non-coding RNA H19 regulates cell growth and metastasis via the miR-22-3p/Snail1 axis in gastric cancer. *Int J Oncol* 2019;54:2157–68.
- [20] Vo DT, Karanam NK, Ding L, et al. miR-125a-5p functions as tumor suppressor microRNA and is a marker of locoregional recurrence and poor prognosis in head and neck cancer. *Neoplasia* 2019;21:849–62.
- [21] Cao Q, Wang N, Ren L, Tian J, Yang S, Cheng H. miR-125a-5p post-transcriptionally suppresses GALNT7 to inhibit proliferation and invasion in cervical cancer cells via the EGFR/PI3K/AKT pathway. *Mol Cancer* 2020;20:117.
- [22] Chen LY, Wang L, Ren YX, et al. The circular RNA circ-ERBIN promotes growth and metastasis of colorectal cancer by miR-125a-5p and miR-138-5p/4EBP-1 mediated cap-independent HIF-1 α translation. *Oncol Rep* 2020;43:1234–44.
- [23] Liu W, Ren H, Ren J, et al. The role of EGFR/PI3K/Akt/cyclinD1 signaling pathway in acquired middle ear cholesteatoma. *Mediators Inflamm* 2013;2013:651207.
- [24] Chen Y, Li C, Tan C, Liu X. Circular RNAs: a new frontier in the study of human diseases. *J Med Genet* 2016;53:359–65.
- [25] Ojha R, Nandani R, Chatterjee N, Prajapati VK. Emerging role of circular RNAs as potential biomarkers for the diagnosis of human diseases. *Adv Exp Med Biol* 2018;1087:141–57.
- [26] Lu D, Thum T. RNA-based diagnostic and therapeutic strategies for cardiovascular disease. *Nat Rev Cardiol* 2019;16:661–74.
- [27] Chen Y, Cai J, Yang FX, Zhou B, Zhou LR. Ascorbate peroxidase from *Jatropha curcas* enhances salt tolerance in transgenic Arabidopsis. *Genet Mol Res* 2015;14:4879–89.
- [28] Ni K, Wang D, Xu H, et al. miR-21 promotes non-small cell lung cancer cells growth by regulating fatty acid metabolism. *Cancer Cell Int* 2019;19:219.
- [29] Ma J, Shang S, Wang J, et al. Identification of miR-22-3p, miR-92a-3p, and miR-137 in peripheral blood as biomarker for schizophrenia. *Psychiatry Res* 2018;265:70–6.
- [30] Ji Q, Wang X, Cai J, Du X, Sun H, Zhang N. MiR-22-3p regulates amyloid β deposit in mice model of Alzheimer's disease by targeting mitogen-activated protein kinase 14. *Curr Neurovasc Res* 2019;16:473–80.
- [31] Chen J, Wu FX, Luo HL, et al. Berberine upregulates miR-22-3p to suppress hepatocellular carcinoma cell proliferation by targeting Sp1. *Am J Transl Res* 2016;8:4932–41.
- [32] Liu Y, Li H, Liu Y, Zhu Z. MiR-22-3p targeting alpha-enolase 1 regulates the proliferation of retinoblastoma cells. *Biomed Pharmacother* 2018;105:805–12.
- [33] Wang M, Chen B, Ru Z, Cong L. CircRNA circ-ITCH suppresses papillary thyroid cancer progression through miR-22-3p/CBL/ β -catenin pathway. *Biochem Biophys Res Commun* 2018;504:283–8.
- [34] Xu L, Li Y, Yin L, et al. miR-125a-5p ameliorates hepatic glycolipid metabolism disorder in type 2 diabetes mellitus through targeting of STAT3. *Theranostics* 2018;8:5593–609.
- [35] Zhang Y, Zhang D, Lv J, Wang S, Zhang Q. MiR-125a-5p suppresses bladder cancer progression through targeting FUT4. *Biomed Pharmacother* 2018;108:1039–47.
- [36] Yan L, Yu MC, Gao GL, et al. MiR-125a-5p functions as a tumour suppressor in breast cancer by downregulating BAP1. *J Cell Biochem* 2018;119:8773–83.
- [37] Sun L, Lian JX, Meng S. MiR-125a-5p promotes osteoclastogenesis by targeting TNFRSF1B. *Cell Mol Biol Lett* 2019;24:23.
- [38] Li T, Wang G. Computer-aided targeting of the PI3K/Akt/mTOR pathway: toxicity reduction and therapeutic opportunities. *Int J Mol Sci* 2014;15:18856–91.
- [39] Aoki M, Fujishita T. Oncogenic roles of the PI3K/AKT/mTOR axis. *Curr Top Microbiol Immunol* 2017;407:153–89.
- [40] Yune TY, Byun JY. Expression of PTEN and phosphorylated Akt in human cholesteatoma epithelium. *Acta Otolaryngol* 2009;129:501–6.